A NEW WEATHER FILTER FOR REDUCING WEATHER EFFECT IN CALCULATING SEA ICE CONCENTRATION FROM AMSR2 DATA

K. Cho [1]*, K. Naoki [1]

[1]Tokai University Research & Information Center, 2-3-23, Takanawa, Minato-ku, Tokyo, 108-8619, Japan, kohei.cho@tokai-u.jp

Commission III, WG III/7

KEY WORDS: passive microwave radiometer, GCOM-W, bootstrap algorithm, atmospheric effect

ABSTRACT:

Ice concentration is one of the most fundamental parameters of sea ice which can be calculated from brightness temperatures measured by passive microwave radiometers such as AMSR2 onboard satellites. However, the presence of atmospheric water vapor, cloud liquid water, etc. is likely to increase the brightness temperatures over open water. As a result, sometimes, certain ice concentrations are calculated over open water covered with heavy clouds. The authors call this kind of area as "false sea ice" and the phenomenon is called the weather effect. In the AMSR2 ice concentration product, a weather filter is used to reduce the weather effect. However, it is known that false sea ice appears occasionally in some areas even in the summertime in AMSR2 ice concentration products. In this study, the authors have modified the original weather filter and added a new weather filter utilizing the following two equations which are TB(23GHzV)<-0.75×(TB(36GHzV)-TB(36GHzH))+253K and TB(36GHzV)-TB(36GHzH) < 57K. If the brightness temperature of the pixel meets the above two equations, we set the ice concentration of the pixel as 0%. By adding the new weather filter, most of the false sea ice that appeared in the ASMR2 ice concentration products could be rejected. JAXA has decided to add this weather filter for producing AMSR2 standard sea ice concentration products.

1. INTRODUCTION

The global distribution of sea ice is quite sensitive to global warming. Thus, the importance of sea ice monitoring is increasing. Since longer wavelength microwaves can penetrate clouds, passive microwave radiometers, such as SSM/I and AMSR2 onboard satellites are powerful tools for monitoring the global distribution of sea ice on a daily basis. Long-term monitoring of sea ice with passive microwave radiometers onboard satellites allows us to monitor the trend of global sea ice distribution (Parkinson et al., 1999; Comiso and Nishio, 2008; IPCC, 2014). However, passive microwave radiometers are not completely cloud-free. More or less, microwave signals emitted from the Earth observed by satellites are affected by the atmosphere. When the open water is covered with heavy clouds, the microwave brightness temperature of the area is likely to increase and become a similar value to that of sea ice. As a result, certain sea ice concentration is calculated in the open water area. This is known as "weather effects" (Gloersen et al., 1986). In this study, we call this kind of area "false sea ice". The weather effects are caused by the presence of atmospheric water vapor, cloud liquid water, rain, and sea surface roughening by winds.

To reduce the weather effects, usually, weather filters are applied (Comiso,1995, Cavalieri et al., 1995). The basic idea of a weather filter is to differentiate false sea ice from true sea ice in the characteristic domain of certain parameters derived from microwave brightness temperatures. However, since false sea ice and true sea ice sometimes overlap in the characteristic domain, a weather filter is not always effective. So, when calculating sea ice area from sea ice concentration data derived from passive microwave radiometers, sea ice concentrations (IC) less than 15% are often rejected (IC=0%) to minimize the weather effects. However, this means that true sea ice concentration areas less than 15% are also rejected. In order to improve the sea ice concentration estimation accuracy, improvement of the weather filter to reduce the weather effects is necessary. The authors have been working on improving the weather filter for years (Cho et al., 2010, Tezuka et al., 2013, Sugiura et al., 2016).

In 2012, JAXA launched the advanced passive microwave sensor AMSR2 on-board GCOM-W satellite. The high accuracy of sea ice concentration calculated from AMSR2 is verified by the authors (Cho et al., 2015, 2020). However, false sea ice still appears in the AMSR2 sea ice concentration product under certain conditions. In this paper, the authors present and verify a new weather filter to reduce the weather effects in AMSR2 sea ice concentration products.

2. TEST SITES AND ANALYZED DATA

2.1 Test Sites

In this study, the Bering Sea, the Sea of Okhotsk, and the Labrador Sea were selected as the test sites for the development and evaluation of the new weather filter. Figure 1 shows the test sites. The Bering Sea is the northmost part of the Pacific Ocean, bounded on the west by Russia and on the east by Alaska. The north part of the ocean is connected to the Arctic Ocean through the Bering Strait. Sea ice begins forming in late November and survives until late May to early June. The Sea of Okhotsk is located on the north side of Japan, and the sea is one of the most southern seasonal sea ice zones in the northern hemisphere. The Labrador Sea is an arm of the northern Atlantic located between Greenland and eastern Canada. In November, sea ice starts to come down to the sea mainly through the Davis Strait and survives until late June. Since large false sea ice areas are occasionally observed in these seas, these test sites were selected.

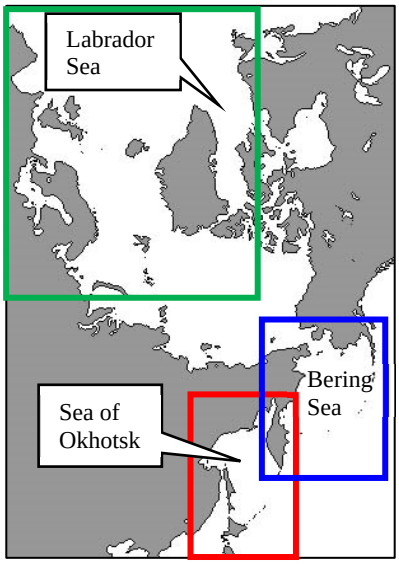

Figure 1. Test Sites

2.2 Analyzed Data

As for the data analysis, the brightness temperatures data measured by the passive microwave radiometer AMSR2 and the sea ice concentration (IC) data derived from the AMSR2 data were used. The sea ice concentrations were calculated using AMSR2 Bootstrap Algorithm (Comiso et. al., 2013).

Table 1. Specifications of AMSR2 (JAXA, 2020)

frequency	resolution	polarization	swath width
7 GHz	35x62 km	Vertical/ Horizontal	1450km
10 GHz	24x42 km		
19 GHz	14x22 km		
23 GHz	15x26 km		
36 GHz	7x12 km		
89 GHz	3x5 km		

3. FALSE SEA ICE

Figure 2 shows the AMSR2 sea ice concentration images of the Bering Sea for the continuous three days from December 29 to 31, 2018. A huge “sea ice area” (indicated by the red circle) is observed on the second day which does not exist on the first day or on the third day. It is not realistic for sea ice to widely appear within one day and disappear next day. This is an example of the “false sea ice” where certain sea ice concentrations were calculated over open water due to the weather effects.

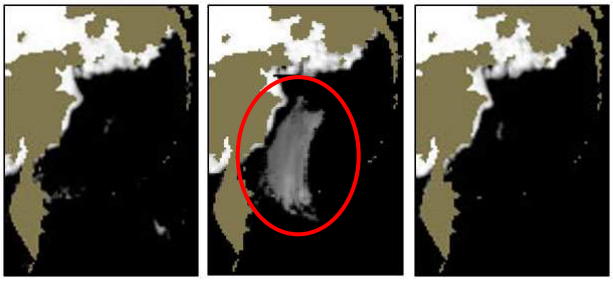

(a) Dec. 29, 2018 (b) Dec. 30, 2018 (c) Dec. 31, 2018

Figure 2. Huge false sea ice area observed in the AMSR2 IC image of the Bering Sea.

4. METHODOLOGY

In sea ice concentration algorithms, such as AMSR2 Bootstrap Algorithm, weather filters are applied to reduce the weather effects. The basic idea of weather filters is to set the sea ice concentration of the pixel to zero when the pixel value meets certain condition. In AMSR2 Bootstrap Algorithm, if the pixel value meets the following equation, the sea ice concentration of the pixel will be set to zero.

$$(TB23V-TB19V) > 19K \quad (1)$$

Where TB23V, TB19V represent brightness temperatures of the vertical polarizations(V) of 23GHz and 19GHz radiometer respectively. Figure 3 shows the idea of the filter displayed on the (TB23GHz-19GHz) vs TB36GHzV domain. The weather filter works well in many cases but not always. As a result, false sea ice as shown on Figure 2(b) occasionally appears in AMSR2 IC images. Fortunately, the number of the cases are not much. However, since large false sea ice appeared in AMSR2 IC images reduce the reliability of the dataset, reduction of weather effect is necessary. To clarify the problem, the authors have selected sample areas of false sea ice, sea ice and open water from the AMSR2 IC image of the test site observed on December 30, 2018 as sown on Figure 4.

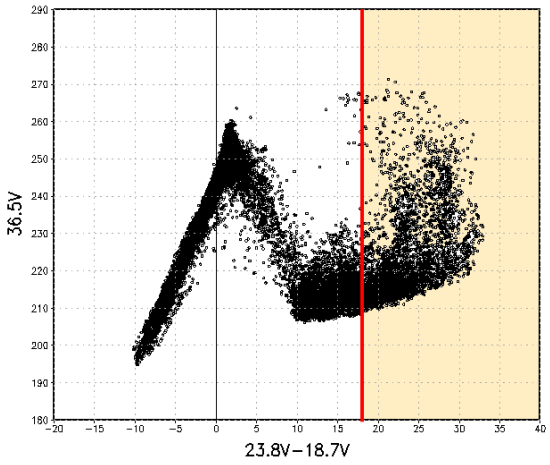

Figure 3. A Weather Filter used in Bootstrap Algorithm (Comiso et al, 1995, 2013)

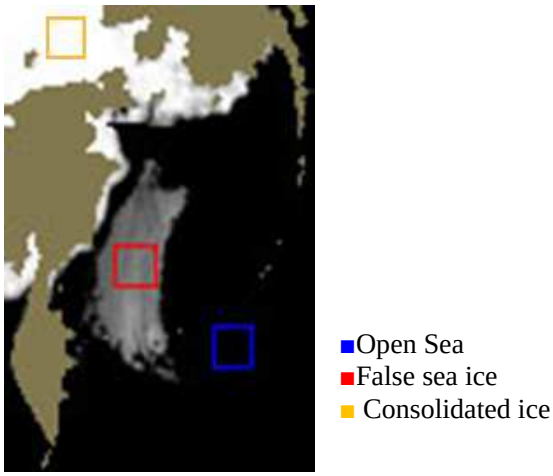

Figure 4. Sample area extraction from AMSR2 IC image (Bering Sea, AMSR2 Dec. 30, 2018)

Figure 5(a) shows the scatter plots of those sample areas of in (TB23V-TB19V) vs (TB23V) domain. pink mesh area indicates the pixels to be rejected as false sea ice. The scatter plot clearly showed that the current weather filter is not working properly for rejecting most of the false sea ice areas of this image. To reject the false sea ice, the authors have changed the threshold level from 18K to 8K (see Figure 5(b)).

$$(TB23V-TB19V) > 7K \quad (2)$$

The result of the threshold change is shown in Figure 6. Though most of the false sea ice was well rejected, the true sea ice areas along the coast of Russia and near Alaska were also rejected. This was because of the true sea ice area which brightness temperature of (TB23V-TB19V) higher than 7K were also rejected.

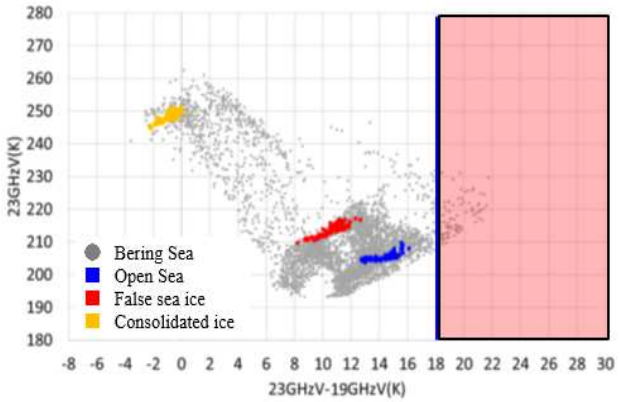

(a) Threshold level=18K

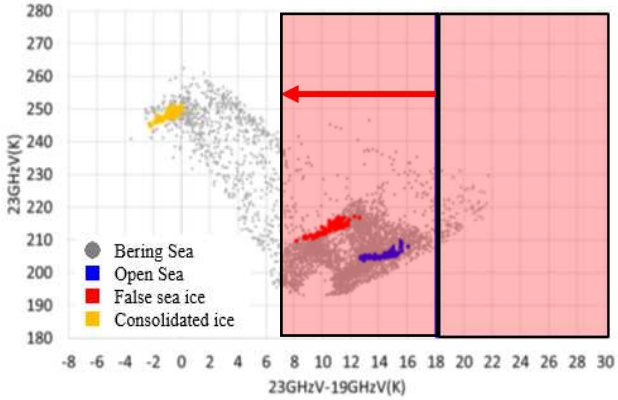

(b) Threshold level=7K

Figure 5. Weather filter threshold setting in the scatter plot of (TB23V-TB19V) vs (TB23V) (Bering Sea, Dec. 30, 2018)

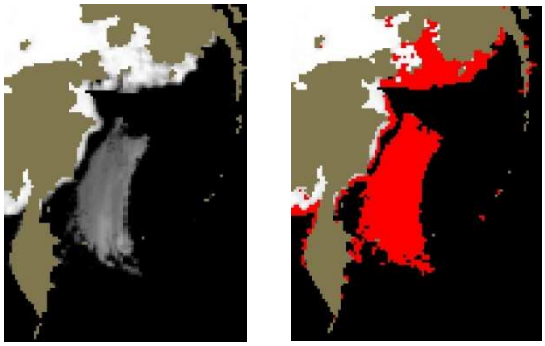

(a)Original IC image (b)Rejected areas are shown in red

Figure 6. False sea ice area rejection with threshold = 7K. (Bering Sea, AMSR2 Dec. 30, 2018)

To solve this problem, the authors have examined various band combinations of AMSR2. Finally, the authors have introduced a new characteristic domain of (TB36V - TB36H) vs TB23V as shown in Figure 7. In this characteristic domain, the false sea ice (shown in red dots) is distributed along a line with open water (shown in blue dots). Considering these kinds of data distribution, the authors have introduced the following two equations to reject false sea ice.

$$(TB36V-TB36H) > 57K \quad (3)$$

$$TB23V + 0.75 \times (TB36V - TB36H) < 250K \quad (4)$$

In the new weather filter, all the pixels that satisfy the equations (2), (3), and (4) are rejected as false sea ice.
Figure 8 shows the result of applying the new weather filter to the previous AMSR2 IC image of the Bering Sea observed on December 30, 2018. The areas colored in red in Figure 8(b) are the false sea ice areas rejected by the new weather filter. Most of the false sea ice areas were well rejected. A small real sea ice area on the ice edge of the upper part of the Bering Sea was also rejected (see green circle). However, since the IC of the rejected pixels was lower than 15%, the result is better than rejecting all the real sea ice pixels whose IC is less than 15%.

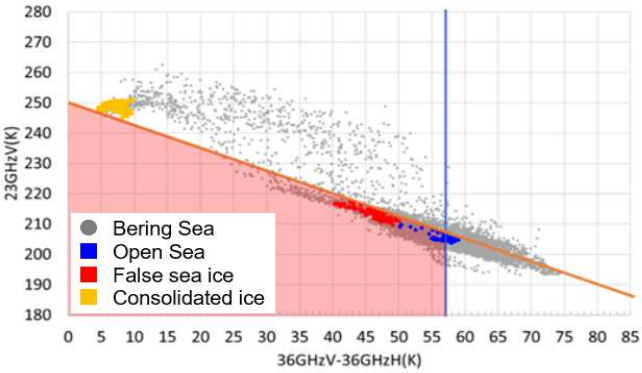

Figure 7. New Weather filter for rejecting the threshold setting in the scatter plot of (TB36V-TB36H) vs (TB23V) (Bering Sea, Dec. 30, 2018)

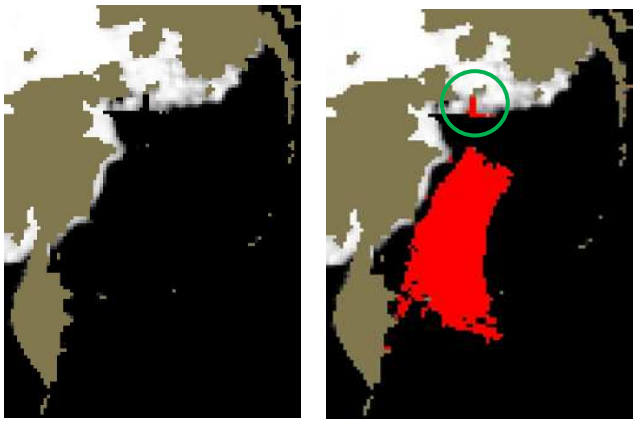

(a)Rejected IC image (b) Rejected area shown in red

Figure 8. False sea ice area rejection result using the new weather filter. (Bering Sea, AMSR2 Dec. 30, 2018)

5. VERIFICATION RESULTS

The authors have applied this method to the other false sea ice-appearing areas as follows.

5.1 Bering Sea

Figure 9(a) shows the AMSR2 IC image of the Bering Sea observed on December 13, 2015. A huge false sea ice area (see red circle) appeared only on this day. The authors selected sample areas of false sea ice, sea ice, and open water from the AMSR2 IC image as shown in Figure 9(b). To clarify the distribution of brightness temperatures of false sea ice, most of the false sea ice areas observed in this image were selected as sample data. Figure 10 shows the scatter plots of those sample areas in (TB23V-TB19V) vs (TB23V) domain and in (TB36V - TB36H) vs TB23V domain. The distributions of sample areas were quite similar to Figures 5 and 7.

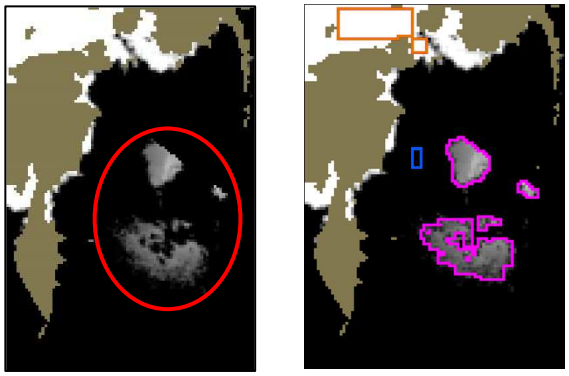

(a) Original IC image (b) Selection of sample areas

Figure 9. Sample area selection from AMSR2 IC image (Bering Sea, AMSR2 Dec. 13, 2015)

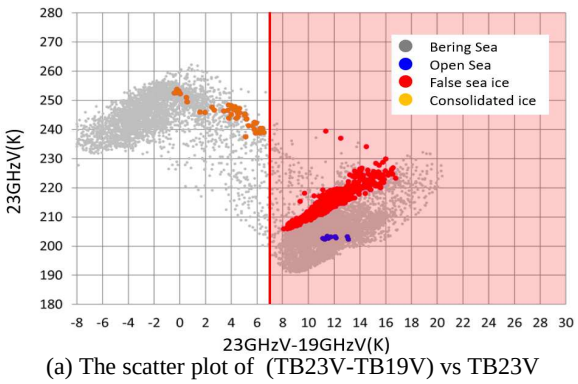

(a) The scatter plot of (TB23V-TB19V) vs TB23V

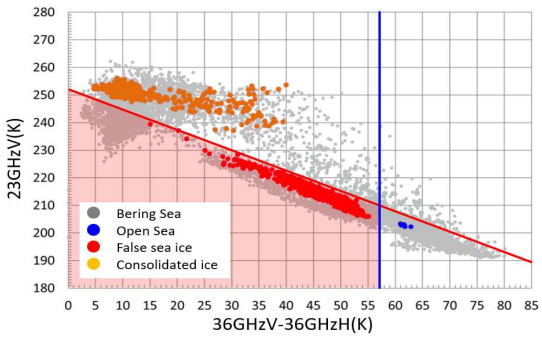

(b) The scatter plot of (TB36V-TB36H) vs TB23V

Figure 10. Weather filter scatter plots (Bering Sea, Dec. 13, 2015)

Figure 11 shows the result of applying the new weather filter to the AMSR2 IC image of the Bering Sea observed on December 13, 2015. The red color areas are the false sea ice areas rejected by the new weather filter. Most of the false sea ice areas were well rejected. A small real sea ice area on the ice edge of the upper part of the Bering Sea was also rejected (see the green rectangle). The zoom-up of the area is shown in Figure 12 with IC values of the rejected pixels. It is clear that the IC value of most of the rejected pixels was lower than 15%.

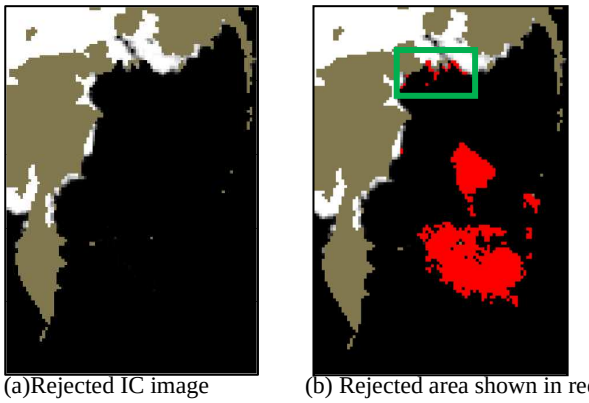

(a)Rejected IC image (b) Rejected area shown in red

Figure 11. False sea ice area rejection result using the new weather filter (Bering Sea, AMSR2 Dec. 13, 2015)

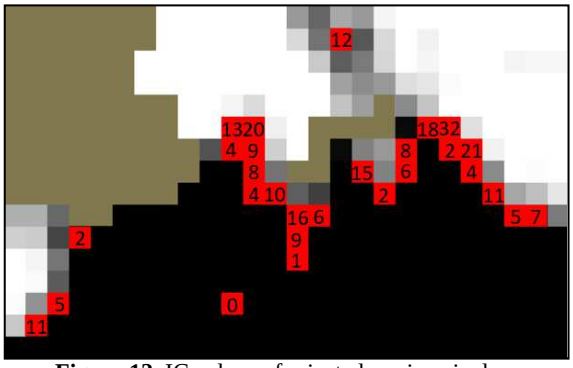

Figure 12. IC values of rejected sea ice pixels (Bering Sea, AMSR2 Dec. 13, 2015)

5.2 Sea of Okhotsk

The new weather was also applied to the false sea ice areas observed in the Sea of Okhotsk as shown on Figure 13. Most of the false sea ice areas were well rejected.

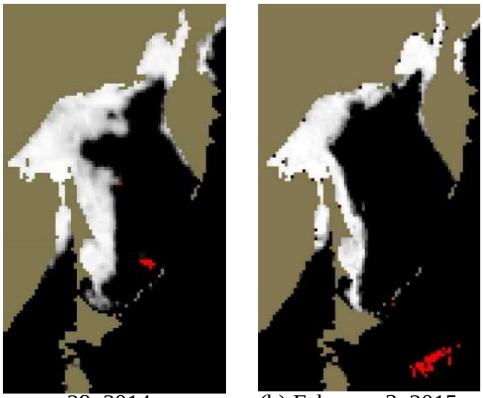

(a) January 29, 2014 (b) February 3, 2015

Figure 13. False sea ice rejection in the Sea of Okhotsk (AMSR2 IC Image)

This contribution has been peer-reviewed. The double-blind peer-review was conducted on the basis of the full paper.
https://doi.org/10.5194/isprs-annals-X-1-W1-2023-793-2023 | © Author(s) 2023. CC BY 4.0 License.

5.3 Labrador Sea

Figure 14 shows the AMSR2 IC images around the Greenland observed from January 23 to 26, 2017. A huge false sea ice area suddenly appeared in the Labrador Sea on January 24 and disappeared within two days. The authors have applied the new weather filter to the data of January 24. The result is shown on Figure 15. Most false sea ice in the Labrador Sea was well rejected. However, again, a small real sea ice area along the ice edge beside Greenland was also rejected (see the green rectangle). The histogram of the rejected pixels is shown in Figure 16. Though the IC values of a few pixels were between 15 to 35%, the IC value of most of the rejected pixels was lower than 15%.

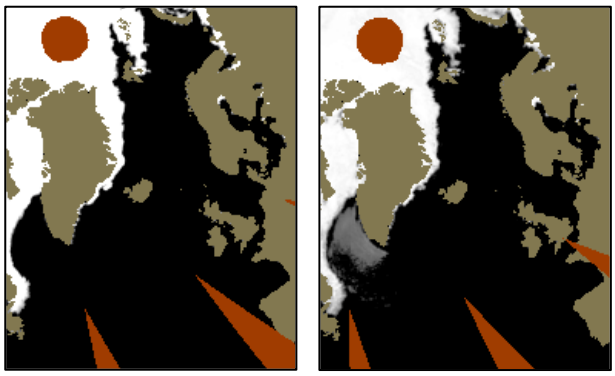

(a) January 23, 2017 (b) January 24, 2017

(c)January 25, 2017 (d) January 26, 2017

Figure 14. Huge false sea ice area observed in the AMSR2 IC image of the Labrador Sea.

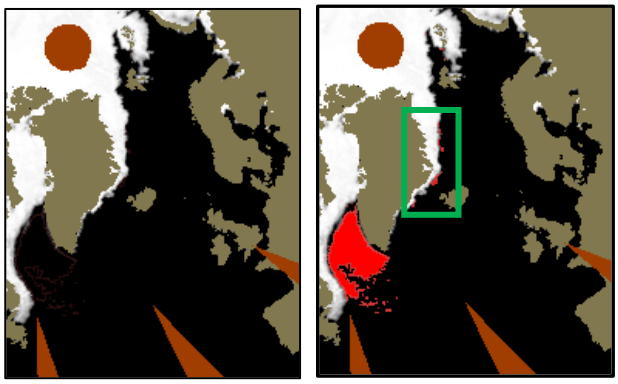

(a)Rejected IC image (b) Rejected area shown in red

Figure 15. False sea ice area rejection result using the new Weather filter (Labrador Sea, AMSR2 Jan. 24, 2017)

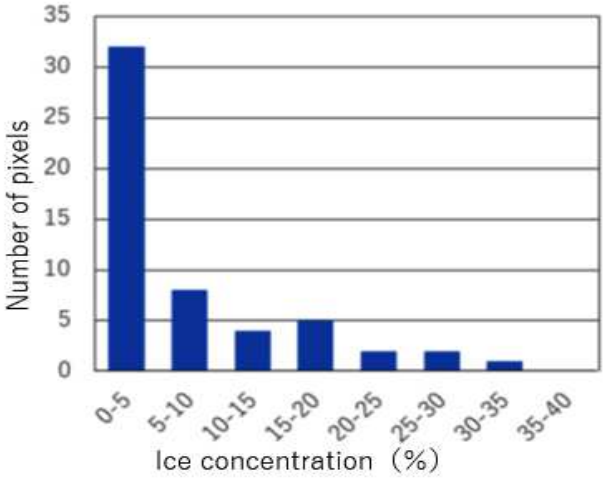

Figure 16. Histogram of the rejected pixels of the true ice along the ice edge of Figure 11.

6. CONCLUSION

The huge false sea ice that appears in AMSR2 IC images does reduce the reliability of the AMSR2 IC dataset. Moreover, false sea ice observed in the AMSR2 IC images may provide the wrong information for ship navigation. In this study, authors have introduced a new weather filter for rejecting false sea ice appearing in the sea ice concentration images of AMSR2. The new weather filter was applied to the AMSR2 IC images of the Bering Sea, Okhotsk Sea, and Labrador Sea for verification. Most of the false sea ice produced by the weather effects was well rejected with the new filter. The rejection of false sea ice may contribute to avoiding the overestimation of sea ice area. It is true that in some cases, some true sea ice areas were also rejected with the filter. The true sea ice rejection may contribute to the underestimation of the sea ice area. However, the number of those pixels was much lower than the number of false sea ice pixels rejected with the filter. Moreover, the IC values of the rejected true sea ice pixels were lower than 35% and mostly less than 15%. As a result, the reduction of the true sea ice area may not have much influence on the calculation of the sea ice extent. Since authors could not find huge false sea ice in the Southern Hemisphere, the new filter was applied only to the Northern Hemisphere and not applied to the Southern Hemisphere. JAXA has decided to utilize this new weather filter at least for producing the future AMSR2 standard sea ice concentration product of the Northern Hemisphere.

ACNORIDGEMENT

This study was performed under the sponsorship of the JAXA 3rd Research Announcement on the Earth Observation (EO-RA3). The support from Ms. Misako Kachi and Dr. Rigen Shimada of JAXA was very helpful. The advice from Dr. Josefino Comiso of NASA was always encouraging. The study was also supported by the past students of Cho Lab. at Tokai University. Without their contribution, the authors could not accomplish this study. The authors would like to thank all of them for their kind support.

REFERENCES

Parkinson, C. L., D. J. Cavalieri, P. Gloersen, H. J. Zwally, and J. C. Comiso, 1999, Arctic sea ice extents, areas, and trends, 1978– 1996, J. Geophys. Res., Vol.104, C9, 20837–20856.

Comiso, J. and F. Nishio, 2008, Trends in the sea ice cover using enhanced and compatible AMSR-E & SMMR, J. Geophys. Res., Vol. 113, C02S07, pp.1-22.

IPCC. 2014. "Summary for Policymakers." *In Climate Change 2013: The Physical Basis*. Contribution of Working Group I to the Fifth Assessment Report of the Intergovernmental Panel on Climate Change, edited by T.F. Stocker, D. Qin, G.K. Plattner, *et al*. Cambridge: Cambridge University Press.

Gloersen, P. and D. J. Cavalieri, 1986, Reduction of weather effects in the calculation of sea ice concentration from microwave radiances, J. Geophys. Res., (l.91)3913-3919.

Comiso, J. C., 1995, SSM/I Sea Ice Concentrations Using the Bootstrap Algorithm, NASA Reference Publication 1380, Maryland, NASA Center for AeroSpace Information, Available online:
http://www.geobotany.uaf.edu/library/pubs/ComisoJC1995_nasa_1380_53.pdf.

Cavalieri, D. J., K. M. St. Germain, and C. T. Swift., 1995, Reduction of weather effects in the calculation of sea ice concentration with the DMSP SSM/I. Journal of Glaciology. (41, 139) 455-464.

Cho K., K. Nishiura, 2010, A study on cloud effect reduction for extracting sea ice area from passive microwave sensor data, The International Archives of the Photogrammetry, Remote Sensing and Spatial Information sciences, Vol. XXXVIII-Part 8, pp.1042-1045.

Tezuka T., K. Cho, 2013, Reduction of Atmospheric Effects in Sea Ice Concentration Estimation Using Satellite Microwave Radiometer AMSR2, Proceedings of the 34th Asian Conference on Remote Sensing, SC01, pp.332-338.

Shu Sugiura, Kazuhiro Naoki, Kohei Cho, 2016, Atmospheric Effect Reduction In Calculating Sea Ice Concentration From AMSR2 Data, Proceedings of the 37th Asian Conference on Remote Sensing, Ab0569, pp.1-4.

Cho K., K. Naoki, 2015, Advantages of AMSR2 for Monitoring Sea Ice from Space, Proceedings of the 36th Asian Conference on Remote Sensing, WE4.8, pp.1-8.

Cho, K., Naoki, K., and Comiso, J. 2020, Detailed Validation of AMSR2 Sea Ice Concentration Data using MODIS Data in The Sea of Okhotsk, ISPRS Ann. Photogramm. Remote Sens. Spatial Inf. Sci., V-3-2020, 369–373, https://doi.org/10.5194/isprs-annals-V-3-2020-369-2020.

Comiso, J. C., K. Cho, 2013, Description of GCOM-W1 AMSR2 Sea Ice Concentration Algorithm, Descriptions of GCOM-W1 AMSR2 Level 1R and Level 2 Algorithms, JAXA, NDX-120015A, (6)1-28, Available online:http://suzaku.eorc.jaxa.jp/GCOM_W/data/doc/NDX-120015A.pdf

JAXA, 2020, http://suzaku.eorc.jaxa.jp/GCOM_W/w_amsr2/amsr2_body_main_j.html,.